

# Analysis of Arabidopsis with Highly Reduced Levels of Malate and Fumarate Sheds Light on the Role of These Organic Acids as Storage Carbon Molecules<sup>1[W]</sup>

Martina B. Zell, Holger Fahnenstich<sup>2</sup>, Alexandra Maier, Mariana Saigo, Elena V. Voznesenskaya, Gerald E. Edwards, Carlos Andreo, Frank Schleifenbaum, Christiane Zell, María F. Drincovich, and Verónica G. Maurino\*

Botanisches Institut, Biowissenschaftliches Zentrum, Universität zu Köln, 50674 Cologne, Germany (M.B.Z., H.F., A.M., V.G.M.); Centro de Estudios Fotosintéticos y Bioquímicos, Universidad Nacional de Rosario, Suipacha 531, Rosario, Argentina (M.S., C.A., M.F.D.); Laboratory of Anatomy and Morphology, V.L. Komarov Botanical Institute of Russian Academy of Sciences, 197376 St. Petersburg, Russia (E.V.V.); School of Biological Sciences, Washington State University, Pullman, Washington 99164–4236 (G.E.E.); and Center for Plant Molecular Biology, Department of Plant Physiology (F.S.), and Institute for Physical and Theoretical Chemistry (F.S., C.Z.), University of Tuebingen, 72076 Tuebingen, Germany

While malate and fumarate participate in a multiplicity of pathways in plant metabolism, the function of these organic acids as carbon stores in C<sub>3</sub> plants has not been deeply addressed. Here, Arabidopsis (*Arabidopsis thaliana*) plants overexpressing a maize (*Zea mays*) plastidic NADP-malic enzyme (ME<sub>m</sub> plants) were used to analyze the consequences of sustained low malate and fumarate levels on the physiology of this C<sub>3</sub> plant. When grown in short days (SD), ME<sub>m</sub> plants developed a pale-green phenotype with decreased biomass and increased specific leaf area, with thin leaves having lower photosynthetic performance. These features were absent in plants growing in long days. The analysis of metabolite levels of rosettes from transgenic plants indicated similar disturbances in both SD and long days, with very low levels of malate and fumarate. Determinations of the respiratory quotient by the end of the night indicated a shift from carbohydrates to organic acids as the main substrates for respiration in the wild type, while ME<sub>m</sub> plants use more reduced compounds, like fatty acids and proteins, to fuel respiration. It is concluded that the alterations observed in SD ME<sub>m</sub> plants are a consequence of impairment in the supply of carbon skeletons during a long dark period. This carbon starvation phenotype observed at the end of the night demonstrates a physiological role of the C<sub>4</sub> acids, which may be a constitutive function in plants.

Fumarate can accumulate to high levels in Arabidopsis (*Arabidopsis thaliana*) and agronomically important C<sub>3</sub> plants like soybean (*Glycine max*) and sunflower (*Helianthus annuus*; Chia et al., 2000; Fahnenstich et al., 2007). It is synthesized from malate through the action of fumarase (Gout et al., 1993). Malate is an intermediate of the tricarboxylic acid (TCA) cycle and a regulator of pH and nutrient uptake and stomatal function (Fernie and Martinoia, 2009). Malate also has an important role in photosynthesis in Crassulacean acid metabolism and C<sub>4</sub> plants (Drincovich et al., 2010). In some C<sub>3</sub> plants like Arabidopsis, malate

and fumarate levels show diurnal changes similar to those of starch and Suc: They increase during the day and decrease during the night, suggesting that they function as transient carbon storage molecules (Fahnenstich et al., 2007). As fumarate is highly concentrated in stems (Stumpf and Burris, 1981) and phloem exudates (Chia et al., 2000), it was proposed that it might also be involved in carbon partitioning. There is variation in the extent to which C<sub>3</sub> plants store photosynthates in the form of sugars and organic acids in leaves during carbon assimilation (Zeeman and Ap Rees, 1999; Chia et al., 2000; Zeeman et al., 2007). In Arabidopsis, approximately half of the photoassimilates are partitioned into starch (Sun et al., 1999; Zeeman and Ap Rees, 1999). Under short days (SD), the partitioning of assimilates to the formation of starch is greater than in long days (LD; Gibon et al., 2004). Thus, the longer the night, the higher is the proportion of photoassimilates stored as starch to provide carbon skeletons during the prolonged dark period.

We recently established transgenic lines of Arabidopsis with decreased malate and fumarate levels by overexpressing a maize (*Zea mays*) plastidic NADP-

<sup>1</sup> This work was supported by the Deutsche Forschungsgemeinschaft (grant nos. MA2379/4–1 and 8–1 to V.G.M.).

<sup>2</sup> Present address: Metanomics GmbH, Tegeler Weg 33, 10589 Berlin, Germany.

\* Corresponding author; e-mail v.maurino@uni-koeln.de.

The author responsible for distribution of materials integral to the findings presented in this article in accordance with the policy described in the Instructions for Authors ([www.plantphysiol.org](http://www.plantphysiol.org)) is: Verónica G. Maurino ([v.maurino@uni-koeln.de](mailto:v.maurino@uni-koeln.de)).

<sup>[W]</sup> The online version of this article contains Web-only data.

[www.plantphysiol.org/cgi/doi/10.1104/pp.109.151795](http://www.plantphysiol.org/cgi/doi/10.1104/pp.109.151795)

malic enzyme (MEm plants; Fahnenstich et al., 2007). This enzyme catalyzes the oxidative decarboxylation of malate rendering pyruvate, CO<sub>2</sub>, and NADPH (Maurino et al., 1996). The MEm plants showed an accelerated dark-induced senescence that could be rescued by supplying Glc, Suc, or malate, suggesting that the lack of a readily mobilized carbon source is likely to be the initial factor leading to the premature induction of senescence in MEm plants. In line with these, malate and fumarate were the only two metabolites whose levels were significantly decreased in the MEm lines after dark incubation and whose levels recover to values similar to wild type after incubation with Glc (Fahnenstich et al., 2007).

In this work we address the question whether malate and fumarate function as storage carbon molecules in the C<sub>3</sub> plant *Arabidopsis* by analyzing the consequences of sustained low levels of these organic acids on the performance of MEm plants growing in different photoperiods. We demonstrate that low malate and fumarate levels do not alter morphology, photosynthetic functions, or growth parameters in LD plants. By contrast, MEm plants suffer from a marked decrease in photosynthetic performance and show reduced biomass and a pale-green phenotype in SD. When grown in SD at the end of the night the wild type showed a shift from carbohydrates as the main substrate for respiration to organic acids, while the MEm lines used more reduced substrates (e.g. fatty acids and proteins) to fuel respiration. The alterations observed in SD point to an impairment in the supply of energy and carbon skeletons during a long night, which supports the proposed physiological roles of malate and fumarate as essential storage carbon molecules in *Arabidopsis*.

## RESULTS

### The MEm Plants Display a Light Regime-Dependent Phenotype

When grown in SDs transgenic plants expressing maize NADP-ME had markedly smaller rosettes than wild type (Fig. 1A) and exhibited lower fresh and dry weight, significantly higher fresh weight to dry weight ratio, and specific leaf area (Supplemental Table S1; Supplemental Fig. S1) and thinner leaf sections (45%–60% of wild type; Fig. 2A) than wild type. These results indicated a reduction in shoot biomass in MEm plants, which was reflected by both a higher water content per leaf area and lower dry matter. There is a dose-response relationship between the intensity of the changes observed and the level of NADP-ME activity, as MEm2 plants that have a 6-fold-higher NADP-ME activity than the wild type (Fahnenstich et al., 2007) showed less-accentuated variations in the phenotype than MEm4 and -5 plants, with 24- and 33-fold-higher NADP-ME activities than the wild type (Fahnenstich et al., 2007). In LD, MEm plants were

indistinguishable from wild type (Figs. 1 and 2; Supplemental Fig. S1; Supplemental Table S1).

The rosettes of SD MEm plants were pale green (Fig. 1A) with decreased total chlorophyll and chlorophyll *a* and *b* contents, but having similar chlorophyll *a/b* ratio to wild type (Supplemental Table S2). No significant differences in chlorophyll contents between the genotypes were found in LD plants (Supplemental Table S2).

Light microscopy observations showed that SD MEm plants have decreased leaf thickness (Fig. 2A) and differences in leaf anatomy (Fig. 2B). Leaves of wild type have homogenous rounded mesophyll cells on the adaxial side and spongy mesophyll on the abaxial side, with eight layers (Fig. 2B). The leaves of MEm5 plants have only up to six layers of mesophyll cells and unlike the wild type, the upper layer consists of palisade-like mesophyll cells while cells of spongy mesophyll are rather loosely arranged (Fig. 2B). The analysis of the ultrastructure of chloroplasts indicated that SD MEm plants have a more crowded thylakoid membrane system than wild type (Fig. 2C), while chloroplast of LD MEm plants were similar to wild type (Fig. 2C). To quantify these observations the PSI to PSII ratio was calculated from the corresponding fluorescence spectra of chloroplasts using living cells. The results indicated no differences in this parameter between the transgenic lines and the wild type in both conditions of growth (Fig. 2D). Moreover, the relative distribution of thylakoids per granum indicated a very similar pattern of distribution in wild-type and MEm plants in both photoperiods (Supplemental Table S3).

### Photosynthetic Characteristics

To obtain more direct physiological evidence for the contrasting responses of MEm plants grown under SD and LD regimes, the photosynthetic capacity and chlorophyll fluorescence emission were measured (Fig. 1B). In LD plants, rates of photosynthesis per leaf area were similar in wild-type and MEm2 plants and slightly lower in MEm5 plants. In SD, MEm2 and -5 plants showed a reduction in photosynthesis compared to wild type (Fig. 1B). This lower CO<sub>2</sub> fixation rate per unit leaf area is in accordance with the thinner leaf sections and the most severe reduction in biomass accumulation observed in SD MEm plants (Fig. 2A; Supplemental Table S1). MEm4 plants showed the same behavior as MEm5 plants (data not shown).

Chlorophyll fluorescence analysis showed that in LD there was no difference between wild-type and MEm plants in the yield of PSII measured with increasing photosynthetic photon flux densities (PPFDs; Supplemental Fig. S2a). However, in SD plants the yield of PSII was lower in MEm than in wild-type plants (Supplemental Fig. S2a). This suggests that in SD MEm plants the photochemistry is reduced along with CO<sub>2</sub> fixation per unit area. No differences in the fraction of closed PSII centers (estimated from  $1 - q_p$ ) were detected, which suggests that changes in the

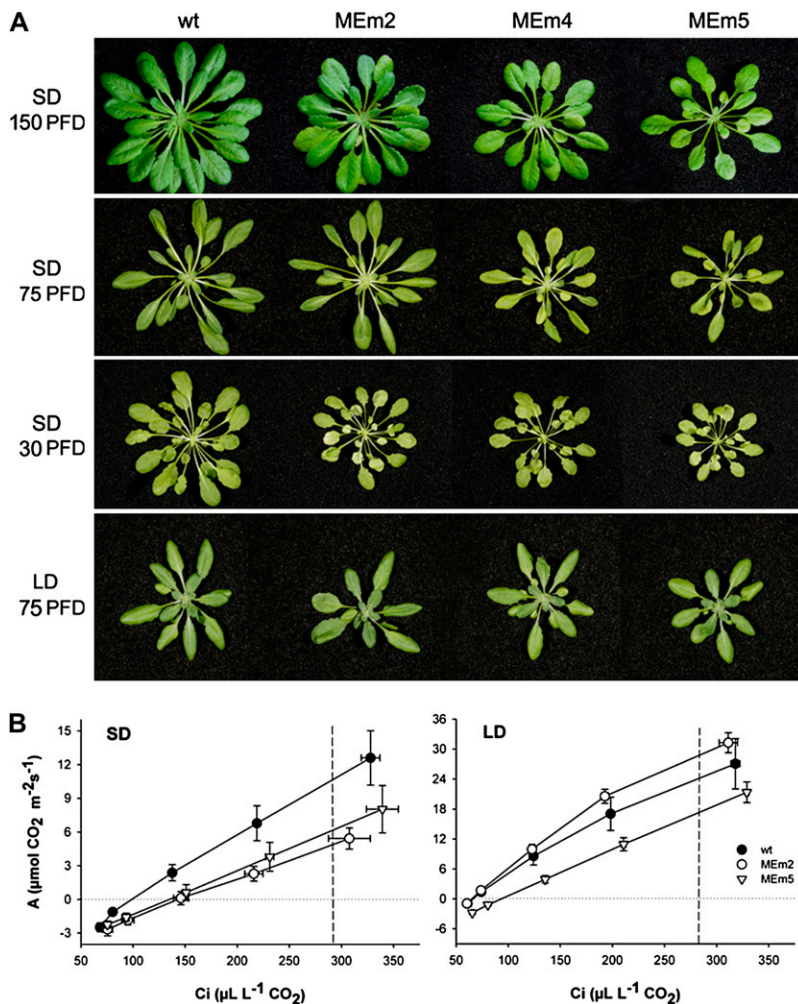


**Figure 1.** Phenotype and photosynthetic performance. A, Representative rosettes of 4-week-old MEm and wild-type (wt) plants grown in LD and 6-week-old plants grown in SD at different PFDs. PFD:  $\mu\text{mol m}^{-2} \text{ s}^{-1}$ . B, Rate of  $\text{CO}_2$  assimilation (A) as a function of the intracellular partial pressure of  $\text{CO}_2$  ( $C_i$ ). Plants were grown at a PFD of  $150 \mu\text{mol quanta m}^{-2} \text{ s}^{-1}$  and the measurements were conducted at a PFD of  $200 \mu\text{mol quanta m}^{-2} \text{ s}^{-1}$ . The dotted lines indicate the  $C_i$  at atmospheric  $\text{CO}_2$  concentrations ( $297$  and  $292 \mu\text{L L}^{-1} \text{ CO}_2$ , in LD and SD grown plants, respectively). Data are means  $\pm$  SE of six plants. The asterisk (\*) indicates significant differences between the values of wild-type and MEm plants calculated by the Student's *t*-test ( $P < 0.05$ ).

redox state on the acceptor side of PSII with increasing light intensity was similar among the genotypes (data not shown).

We further investigated the inactivation of PSII under high-light treatment as an indicator of photo-inhibition of photosynthesis. For this purpose, the time course of the maximum photochemical efficiency of PSII in the dark-adapted state ( $F_v/F_m$ ) ratio was determined as an indication of the maximum quantum efficiency of PSII primary photochemistry. All lines grown at moderate PFD under both SD and LD conditions showed no initial differences in  $F_v/F_m$  (Supplemental Fig. S2b). After exposure to high PFD ( $700 \mu\text{mol m}^{-2} \text{ s}^{-1}$ ),  $F_v/F_m$  of MEm plants showed a drastic decrease after 5 h of treatment followed by a recovery phase in both SD and LD plants (Supplemental Fig. S2b), where SD plants showed a slower recovery phase and then  $F_v/F_m$  declined again (Supplemental Fig. S2b). In the wild type,  $F_v/F_m$  slightly decreased after 5 h in high light and recovered after 2 d (Supplemental Fig. S2b). These results indicate that MEm plants have lower capacity to use higher levels of PFD in photochemistry, and/or that they have

reduced means of photoprotection and preventing inactivation of PSII, especially in SD.

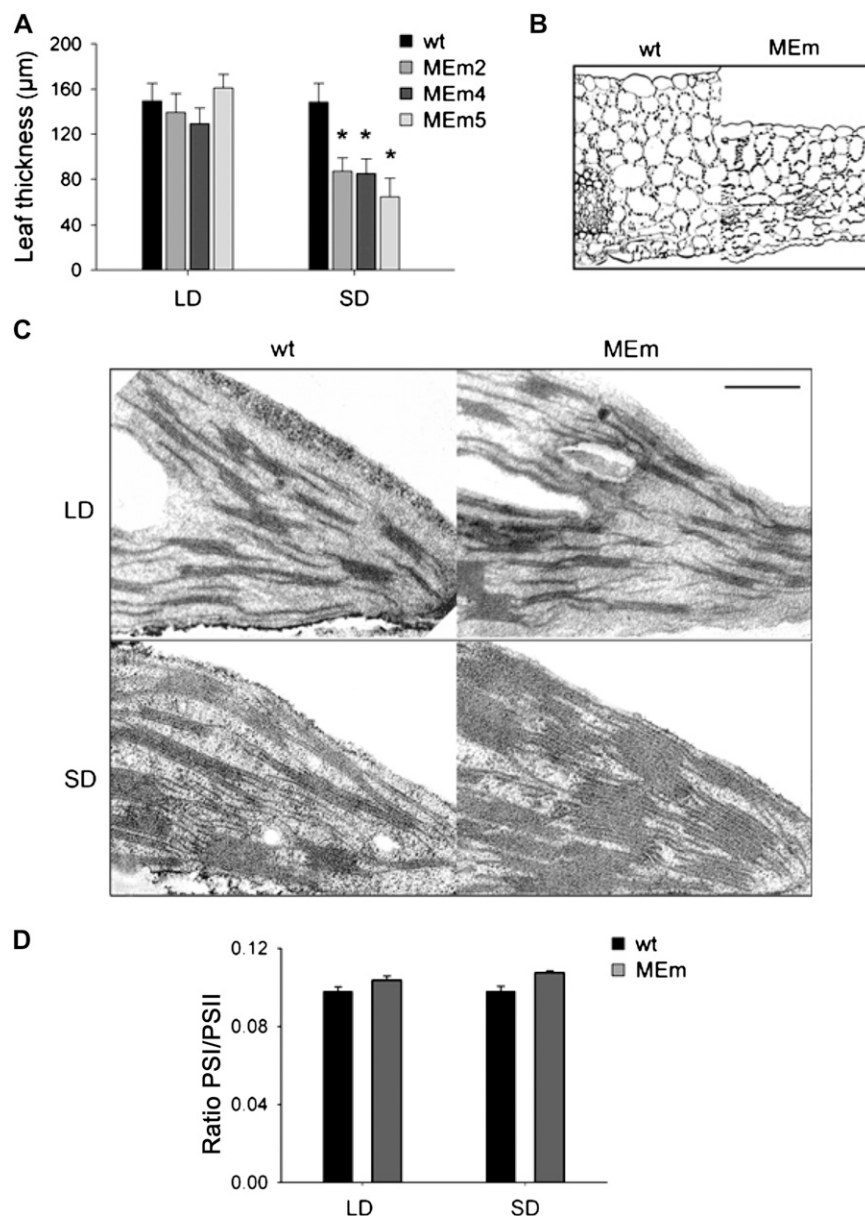
#### Metabolite Analysis

We next determined the levels of soluble sugars, starch and malate photometrically and carried out a metabolite fingerprinting study using gas chromatography-mass spectrometry (GC-MS). As in the case of other parameters, the overexpressing lines MEm4 and -5 showed more pronounced variations in the metabolite profiles compared to wild type, while line MEm2 had an intermediate behavior between wild type and the other MEm lines. In Figures 3 and 4, for ease of comparison, data obtained for MEm2 and -5 plants are shown (also see Supplemental Tables S4 and S5).

#### Carbohydrates and Derivates

Different patterns of soluble sugars accumulation were observed in the wild type grown in SD at different light intensities. At moderate PFD ( $150 \mu\text{mol m}^{-2} \text{ s}^{-1}$ ) the levels of these sugars increased during the day and

**Figure 2.** Leaf thickness and chloroplast ultrastructure. A, Leaf thickness was measured from transverse leaf sections prepared from LD and SD plants grown at a PFD of  $75 \mu\text{mol m}^{-2} \text{s}^{-1}$ . Error bars indicate the SD ( $n = 80$  sections from at least 10 individual plants). The asterisk (\*) indicates significant differences between the values of wild-type (wt) and MEm plants calculated by the Student's *t* test ( $P < 0.05$ ). B, Light microscopy of leaf cross section of SD wild-type and MEm5 plants. Analyzed sections were stained for polysaccharides. The bar represents  $100 \mu\text{m}$ . C, Transmission electron micrographs of chloroplasts of plants grown in LD and SD. Bars represent  $0.5 \mu\text{m}$ . D, PSI to PSII ratio calculated from the corresponding fluorescence spectra of chloroplasts using leaves of 3-week-old plants. Error bars indicate the SE of 40 independent measurements.



decreased during the night (Fig. 3A). In contrast, at low PFD ( $30 \mu\text{mol m}^{-2} \text{s}^{-1}$ ), the levels of these sugars remained low during the whole day-night cycle (Fig. 3A). No significant differences in the accumulation patterns of Glc, Fru, and Suc were observed in the MEm plants compared to wild type (Fig. 3A).

The pattern of starch accumulation of plants grown in SD at moderate PFD indicated similar maximal levels in MEm and wild-type plants with a shift of the maximum starch level to 1 h after darkening in MEm plants (Fig. 3B). In this condition, the average rates of starch synthesis and degradation were similar in MEm and wild-type plants, respectively (Table I). MEm plants grown at low PFD showed a significant higher starch accumulation capacity during the day and higher rate of starch degradation during the night,

reaching similar levels as the wild type at the end of this period (Fig. 3B; Table I).

#### Glycolytic Intermediates and Derivates

The level of pyruvate, the product of the NADP-ME reaction, was enhanced in SD MEm plants, especially during the day (Fig. 4; Supplemental Tables S4 and S5). The pyruvate-derived amino acids Ala, Val, and Leu followed a similar pattern of accumulation and were significantly more abundant in MEm plants, predominantly in the lines with higher NADP-ME activities (Fig. 4; Supplemental Tables S4 and S5).

Glycerate and 3-phosphoglycerate (3-PGA) accumulation profiles were similar in MEm and wild-type plants with a trend to higher glycerate accumulation in

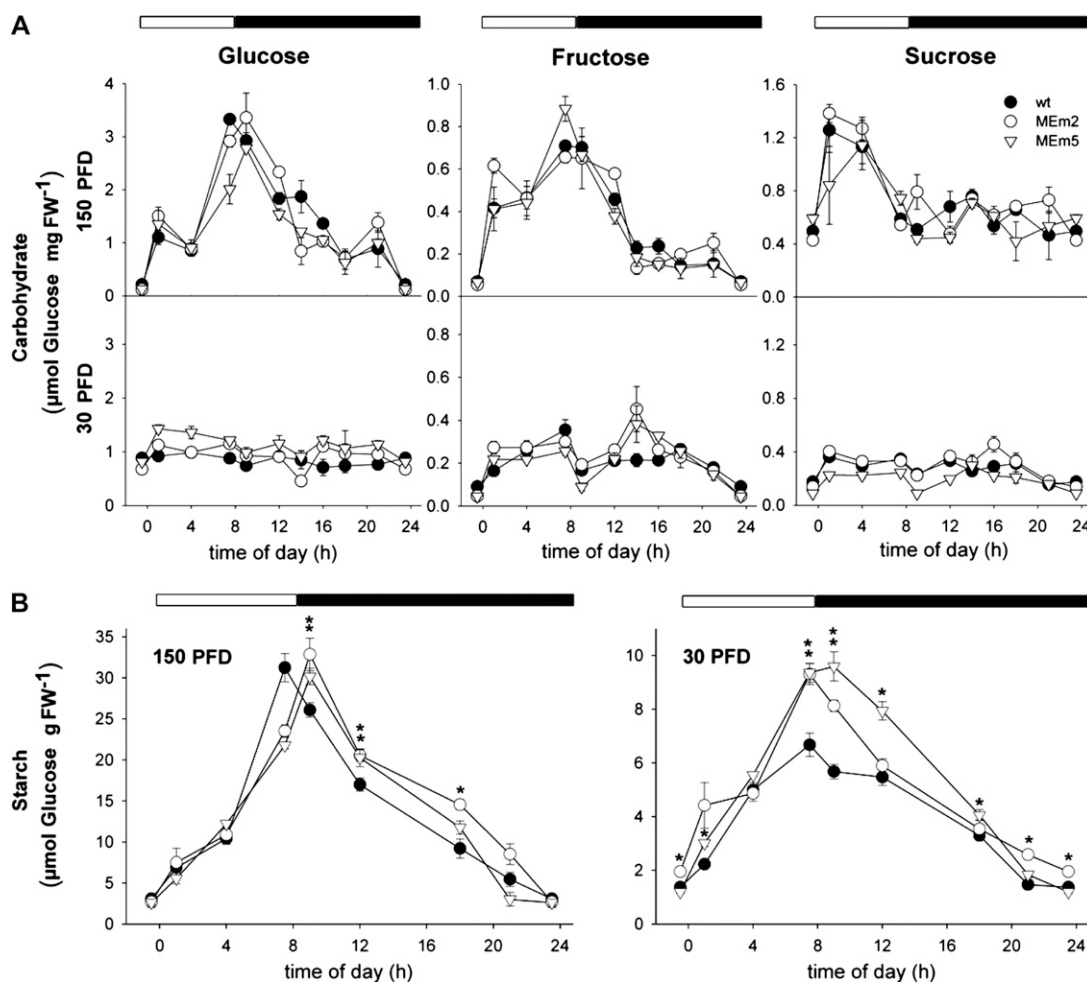


**Figure 3.** Diurnal changes of carbohydrates in rosettes of plants grown in SD at PFDs of 150 and 30  $\mu\text{mol m}^{-2} \text{s}^{-1}$ . A, Diurnal changes of soluble sugars determined photometrically. Values represent the mean  $\pm$  SE of four replicates of eight plants each. In each graphic the onset of the light period was set to  $t = 0$  h. The night period is highlighted with black bars. wt, Wild type. B, Diurnal changes of starch content. Values represent the mean  $\pm$  SE of four replicates of eight plants each. In each graphic the onset of the light period was set to  $t = 0$  h. The dark period is highlighted with black bars. The asterisk (\*) indicates significant differences between the value of the wild-type and MEm plants calculated by the Student's  $t$  test ( $P < 0.05$ ). PFD:  $\mu\text{mol m}^{-2} \text{s}^{-1}$ . FW, Fresh weight.

MEm lines during the light period (Supplemental Tables S4 and S5). The 3-PGA-derived amino acid Ser showed higher accumulation in MEm plants, particularly at moderate PFD (Fig. 4; Supplemental Tables S4 and S5). Possibly, the high content of pyruvate in the MEm plants reduces the flux from 3-PGA to pyruvate and, as a consequence, increase metabolism of PGA to glycerate and Ser.

#### TCA Cycle Intermediates and Derivatives

The organic acids involved in the TCA cycle showed informative patterns of accumulation. Citrate levels were similar in all genotypes at low PFD but at moderate PFD a significant accumulation was observed in MEm lines compared to wild type at the end of the light period (Supplemental Tables S4 and

S5). Under both growth conditions, 2-oxoglutarate showed a higher accumulation in MEm lines (Fig. 4). However, no significant differences in the accumulation of Glu and the Glu-derived metabolites, Gln and GABA, were observed between the lines (Supplemental Tables S4 and S5). Succinate contents in MEm5 showed contrasting variations in both light conditions. At low PFD, the accumulation during the night period was lower than that of wild type and at moderate PFD the accumulation was higher by the end of the light period (Supplemental Tables S4 and S5).

In MEm plants malate and fumarate were drastically decreased at both light conditions during the whole light-dark cycle, especially in the plants with higher NADP-ME activity (Fig. 4; Supplemental Tables S4 and S5). Similar results were obtained by

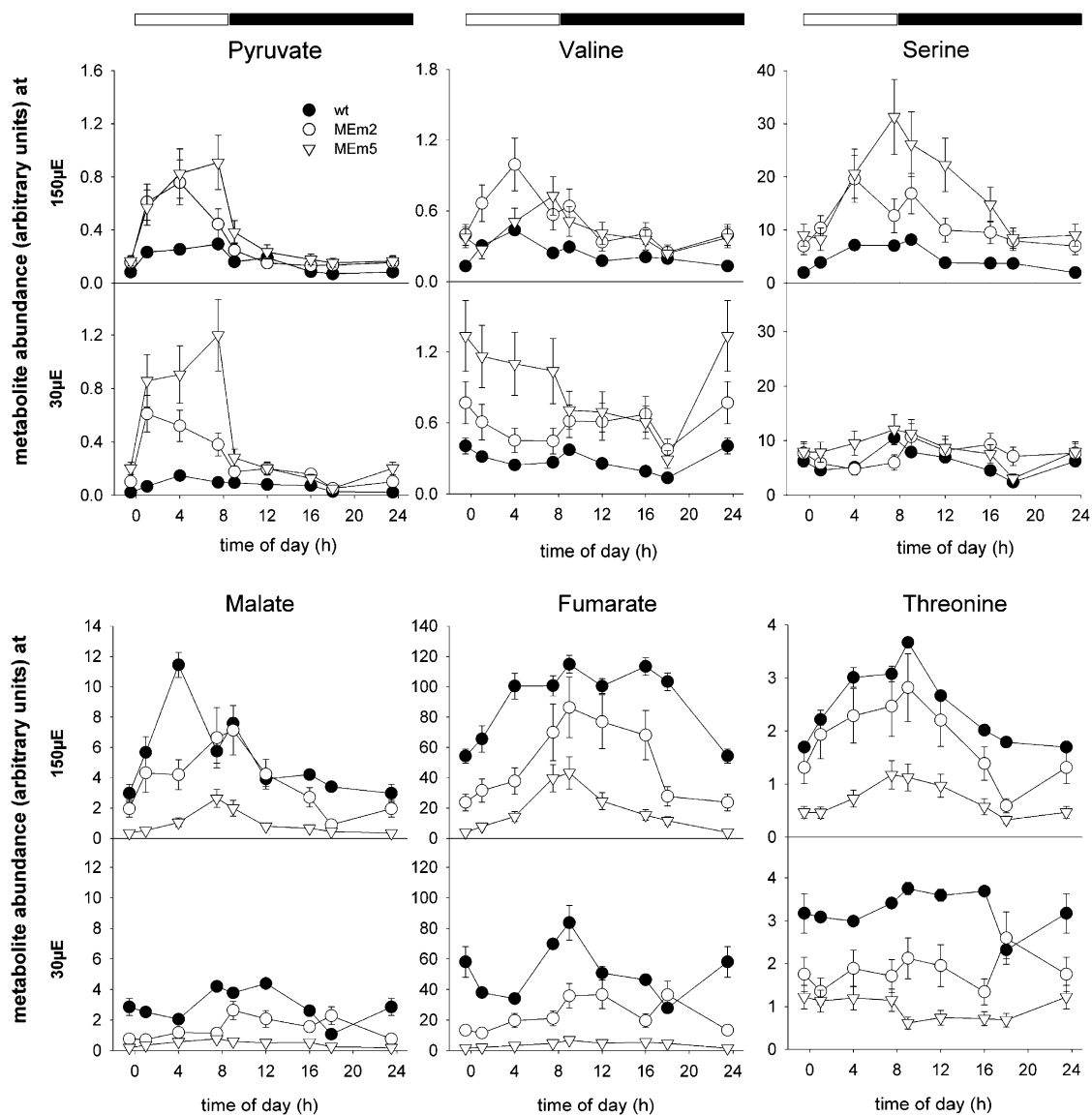


**Figure 4.** Diurnal changes of selected metabolites assayed by GC-MS in rosettes of plants grown in SD at PFDs of 150 and 30  $\mu\text{mol m}^{-2} \text{s}^{-1}$ . The metabolite abundance is presented relative to the internal standard (ribitol) and was calculated as the mean  $\pm$  SE of four replicates of eight plants each. In each graphic the onset of the light period was set to  $t = 0$  h. The dark period is highlighted with black bars. Supplemental Tables S4 and S5 show the time points at which the samples were taken and include the results of the Student's  $t$  test ( $P < 0.05$ ). PFD:  $\mu\text{mol m}^{-2} \text{s}^{-1}$ . wt, Wild type.

measuring the concentrations of malate photometrically (Table II).

Oxaloacetate (OAA)-derived amino acids such as Asp and Thr showed significant lower accumulation in MEm lines during the whole day-night cycle particularly in plants grown at low PFD (Fig. 4; Supplemental Tables S4 and S5), which may reflect a lower content of the precursor OAA due to lower malate and fumarate levels.

#### Pyridine Nucleotide Pool Sizes

Since the NADP-ME reaction involves the reduction of NADP to NADPH, the levels of these nucle-

otides were determined. The average ratio of NADP to NADPH was similar in all genotypes at the end of the light period under LD and SD conditions (Fig. 5A). On the contrary, some differences were observed at the end of the night. When the plants were grown in LD, MEm5 plants showed a higher NADP to NADPH ratio (Fig. 5B) due to lower NADPH levels (data not shown). When the plants were grown in SD at 150  $\mu\text{mol m}^{-2} \text{s}^{-1}$ , all transgenic lines showed significantly lower NADP to NADPH ratios (Fig. 5B) while at 75 and 30  $\mu\text{mol m}^{-2} \text{s}^{-1}$ , the transgenic lines with higher NADP-ME activity showed significantly lower NADP to NADPH ratios

**Table I.** Rate of starch synthesis and degradation calculated as the difference between the maximal and minimal starch concentration divided by the length of the period in h

The plants were grown under SD at a PFD of 30 versus 150  $\mu\text{mol quanta m}^{-2} \text{s}^{-1}$ . Values represent the mean  $\pm$  SE of four replicates of eight plants each. Those that are significantly different from the respective wild type (wt) as determined by the Student's *t* test ( $P < 0.05$ ) are printed in bold.

Genotype	Rate of Synthesis		Rate of Degradation	
	30 PFD	150 PFD	30 PFD	150 PFD
	$\mu\text{mol Glc g fresh weight}^{-1} \text{ h}^{-1}$			
wt	0.663 $\pm$ 0.058	3.176 $\pm$ 0.379	0.331 $\pm$ 0.029	1.588 $\pm$ 0.189
MEM2	<b>0.919 <math>\pm</math> 0.059</b>	3.349 $\pm$ 0.261	<b>0.460 <math>\pm</math> 0.029</b>	1.884 $\pm$ 0.147
MEM5	<b>1.050 <math>\pm</math> 0.063</b>	3.061 $\pm$ 0.096	<b>0.525 <math>\pm</math> 0.031</b>	1.722 $\pm$ 0.054

(Fig. 5B). In all cases, the deviations were exclusively due to lower NADP concentrations (data not shown). The NADP to NADPH ratios of MEM4 resembled those of MEM5 plants in all conditions tested (data not shown).

The contents of NAD and NADH were analyzed at moderate PFD. When the plants were grown in LD, no differences were observed between the genotypes, except for a higher NAD to NADH ratio in MEM2 plants (Fig. 5C), due to a lower accumulation of NADH (data not shown). On the contrary, MEM5 plants presented significantly lower levels of both NAD and NADH (data not shown). In SD conditions, all MEM lines showed significantly lower NAD to NADH ratios at the end of the night (Fig. 5C) due to lower NAD levels and constant NADH levels (data not shown). No differences in the ratio were found at the end of the light period (Fig. 5C). The NAD to NADH ratios of MEM4 resembled those of MEM5 plants in all conditions tested (data not shown).

### Substrates Used for Respiration

To investigate whether the extremely low levels of malate and fumarate affect the energetic metabolism of the MEM plants the respiratory quotient (RQ) was determined. Determination of the RQ is useful because the volumes of  $\text{CO}_2$  released and  $\text{O}_2$  consumed by the leaves depend on which fuel source is being metabolized for respiration (Hurth et al., 2005). At the end of the day in both SD and LD the RQs of all genotypes were close to 1.0 ( $0.93 \pm 0.08$  to  $1.14 \pm 0.13$ ), indicating the use of carbohydrates to fuel respiration. At the end of the night in SD the wild type showed RQs of  $1.86 \pm 0.14$ , indicating a shift from carbohydrates to organic acids as the main substrates for respiration. On the contrary, the MEM2 and -5 plants presented RQs of  $0.34 \pm 0.09$  and  $0.41 \pm 0.07$ , respectively, clearly indicating the use of more reduced carbon sources like lipids and proteins as substrate to fuel respiration. In LD conditions all genotypes presented RQs between  $0.80 \pm 0.10$  and  $1.10 \pm 0.06$ , indicating the primary use of carbohydrates to support respiration at the end of the night.

## DISCUSSION

### Growth and Morphological Modifications in SD MEM Plants

Malate and fumarate participate in a wide number of metabolic pathways. Here, we addressed the question whether these organic acids function as important carbon stores in Arabidopsis. The results obtained demonstrate that high plastidic NADP-ME activity causes a phenotype that is very pronounced under conditions of long nights (16-h darkness) combined with low PFDs during the day. MEM plants grown under SD are pale green, display reduced photosynthetic performance, and produce less biomass. The higher specific leaf area of these plants is a consequence of decreased leaf thickness, which is accompanied by an altered leaf anatomy (Fig. 2). Moreover, the chloroplasts of MEM plants have a more crowded thylakoid membrane system but similar development of grana stacking and PSI to PSII ratios as wild type. This is in strong contrast to numerous reports demonstrating that low-chlorophyll-containing chloroplasts contained less thylakoids (Hugly et al., 1989; Takeuchi et al., 2000; Reiser et al., 2004). Takeuchi et al.

**Table II.** Concentration of malate at the end of the day and night determined photometrically in whole rosettes from plants grown in SD at PFDs of 150 and 30  $\mu\text{mol quanta m}^{-2} \text{s}^{-1}$ 

All values are presented as the mean  $\pm$  SE of four separate samples of eight plants each. Those that are significantly different from the respective wild type (wt) as determined by the Student's *t* test ( $P < 0.05$ ) are printed in bold. PFD:  $\mu\text{mol m}^{-2} \text{s}^{-1}$ .

Growth Condition and Genotype	Malate	
	End Day	End Night
	$\mu\text{mol mg fresh weight}^{-1}$	
150 PFD		
wt	6.45 $\pm$ 0.51	3.40 $\pm$ 0.39
MEM2	4.12 $\pm$ 0.32	2.07 $\pm$ 0.52
MEM5	2.55 $\pm$ 0.23	<b>0.24 <math>\pm</math> 0.05</b>
30 PFD		
wt	4.37 $\pm$ 0.54	3.47 $\pm$ 0.68
MEM2	<b>1.69 <math>\pm</math> 0.20</b>	<b>1.35 <math>\pm</math> 0.08</b>
MEM5	<b>0.62 <math>\pm</math> 0.18</b>	<b>0.15 <math>\pm</math> 0.08</b>



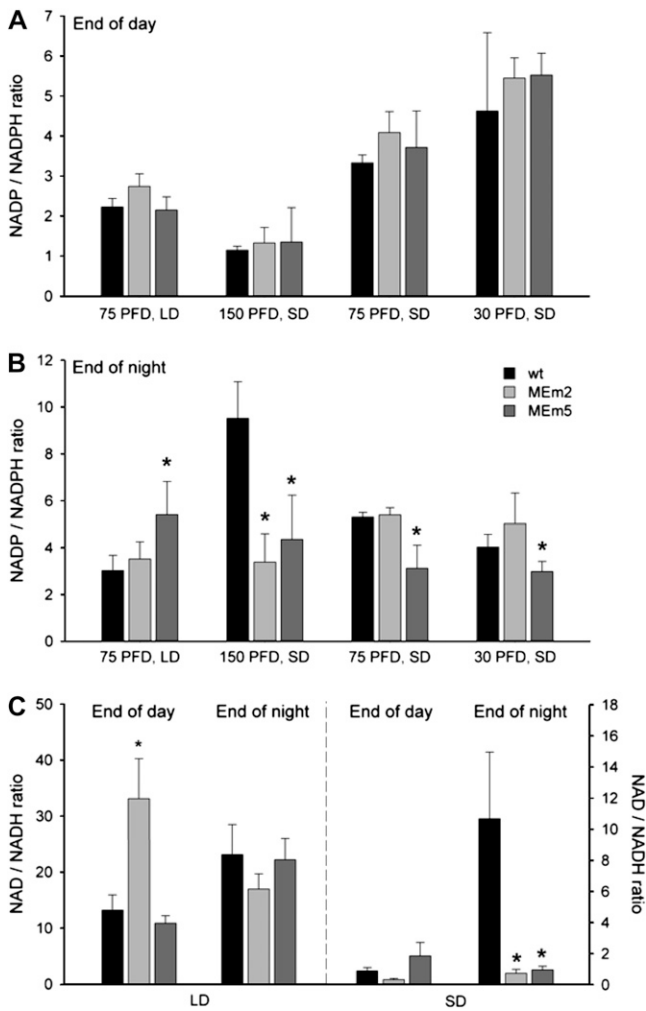


**Figure 5.** Ratio of pyridine nucleotide pool sizes. A and B, NADP to NADPH ratio at the end of the day (A) and night (B) in leaves of plants grown in LD at a PFD of  $75 \mu\text{mol m}^{-2} \text{s}^{-1}$  and SD at 150, 75, and  $30 \mu\text{mol m}^{-2} \text{s}^{-1}$ . Error bars indicate the sds ( $n =$  four independent extracts from eight individual plants). wt, Wild type. C, NAD to NADH ratio at the end of the day and night in leaves of plants grown in LD and SD at moderate PFD. Error bars indicate the sds ( $n =$  four independent extracts from eight individual plants). PFD:  $\mu\text{mol m}^{-2} \text{s}^{-1}$ . The asterisk (\*) indicates significant difference between the values of wild-type and MEm plants calculated by the Student's  $t$  test ( $P < 0.05$ ).

(2000) postulated that as in the case of the bundle sheath chloroplasts of NADP-ME-type  $C_4$  species like maize, the overexpression of NADP-ME in rice (*Oryza sativa*) chloroplasts generated an alternative source of NADPH in the stroma and caused development of agranal chloroplasts. Our results clearly show that a strong expression of NADP-ME in the chloroplasts does not necessarily produce agranal chloroplasts. This may be a feature of rice, which cannot be translated to other unrelated plant species. The actual causes of contrasting ultrastructures of Arabidopsis and rice chloroplast overexpressing the  $C_4$  maize NADP-ME remain unclear and deserve further

elucidation. Nevertheless, it is possible that in SD MEm plants the decreased leaf thickness and thus, the lower chlorophyll content and photosynthetic performance per area might be sensed and as a consequence the plants may adapt the chloroplasts to increase their efficiency for the collection of light by developing a more crowded thylakoid membrane system.

#### Growth of MEm Plants Under SD Results in Lower Photosynthetic Performance and Decreased NADP and NAD Pool Sizes during the Night

The carbon assimilation rate and efficiency of PSII photochemistry in SD MEm plants were decreased, indicating a lower capacity for photosynthesis. No changes in the  $1 - q_p$  parameter and thus, no changes in the redox state of the acceptor side of PSII were observed in MEm plants. Consistent with this, the NADP to NADPH ratio (a primary control of acceptance of electrons from photochemistry) was unaltered during the light period in all genotypes. Overall, these results indicate that the transgenic NADP-ME activity does not cause an overreduction of NADP in Arabidopsis, and thus no overreduction of the electron carriers in photochemistry. For SD-grown wild-type Arabidopsis plants, a high capacity for the safe removal of excess electrons due to an increased NADP-malate dehydrogenase (MDH) activity and higher glutathione contents were reported (Becker et al., 2006). Moreover, Arabidopsis lacking chloroplastic NADP-MDH show no visible differences with the wild type even in high light intensities, indicating that other mechanisms are responsible for the adjustment of redox homeostasis (R. Scheibe, personal communication). This increased metabolic flexibility is likely to be realized in Arabidopsis but obviously not in rice plants overexpressing maize NADP-ME, which showed photoinhibition characteristics triggered by the accumulation of NADPH in the chloroplasts even under normal growth conditions (Takeuchi et al., 2000).

Determination of pyridine nucleotide pool sizes indicated a light regime-dependent and light intensity-dependent decrease in the NADP and NAD levels occurring exclusively in the dark phase. These changes may be the result of mechanisms operating to try to maintain redox homeostasis or decreased synthesis of the nucleotide pools (Noctor et al., 2006). Available data suggest that the first three steps of the de novo NAD biosynthesis involve the production of quinolinate inside the chloroplasts. The first enzyme of this pathway is Asp oxidase, which catalyzes the FAD-dependent oxidation of Asp to iminoaspartate. FAD is regenerated by molecular oxygen or, alternatively, by fumarate (Noctor et al., 2006). In MEm plants the variations in nucleotide pool sizes in SD correlate with extremely low levels of fumarate, suggesting that an impaired regeneration of the redox state of FAD could be involved in a lowered synthesis of NAD and NADP in these conditions.



### Light Regime-Dependent Modifications in the Accumulation and Degradation of Storage Carbon Molecules

The duration of the photoperiod is decisive for many plant responses (Koornneef et al., 1998; Becker et al., 2006). Here, we aimed to study the influence of the photoperiod and the light intensity on the accumulation of selected metabolites of the primary metabolism during a whole day-night cycle by measuring their steady-state levels in rosettes of plants in the middle of the vegetative phase.

In some species, as a result of photosynthesis, sugars and organic acids are produced to varied extent and either stored during the day or allocated to nongreen tissues (Geiger and Servaites, 1994; Zeeman and Ap Rees, 1999; Chia et al., 2000; Zeeman et al., 2007). In the dark, the flux of malate toward the vacuole is stopped and stored fumarate and malate can be released and utilized by the mitochondria through NAD-MDH generating OAA and NAD-ME generating pyruvate feeding into the TCA cycle (Fig. 6; Tronconi et al., 2008). Pyruvate can be used as an energy source in the TCA cycle (Martinoia and Rentsch, 1994) and high levels may up-regulate the respiratory oxygen consumption rate because it can induce alternative oxidase (Vanlerberghe et al., 1999; Oliver et al., 2008; Zabalza et al., 2009). This keto acid can also serve as a precursor for the synthesis of Ala, Val, and Leu.

In the light pyruvate increases, and both pyruvate and CO<sub>2</sub> are products of the NADP-ME reaction. MEM plants showed a similar increase in dark respiration rates measured during the day in both conditions of growth (wild type, MEM2, and MEM5 have dark respiration rates of 2.0, 2.8, and 3.2 in SD and 2.0, 2.5, and 2.8 in LD, respectively). The increase in dark

respiration in the MEM plants may occur due to elevated levels of pyruvate, and some activity of NADP-ME in the chloroplast. It might be argued that an increase of pyruvate and/or of CO<sub>2</sub> production in the chloroplasts of MEM plants and effects in the light could be related to the phenotypical changes observed in MEM plants in SD. In MEM plants, pyruvate levels are higher during the day in both SD and LD, with similar relative maximal levels of accumulation with regards to the wild type in both conditions of growth (Supplemental Table S4; Fahnenstich et al., 2007). Moreover, during the night, the levels of pyruvate rapidly decrease in both conditions following a pattern similar to the wild type (Fahnenstich et al., 2007). Thus, these results suggest pyruvate itself is not a part of the signaling or metabolic effect responsible for the distinctive phenotype of MEM plants growing in SD.

In *Arabidopsis* wild-type plants grown in SD or LD at moderate light intensities, the levels of soluble sugars and the organic acids malate and fumarate increased rapidly after the onset of light and are consumed during the next dark period (Figs. 3 and 4; Fahnenstich et al., 2007). On the contrary, at low PFD these metabolites remain at low levels during the whole cycle (Figs. 3 and 4). Given that in SD the photosynthetic period is reduced, the rate of starch synthesis is increased and that of degradation is decreased to fulfill the carbon demand until the end of the night (Stitt et al., 1978; Gibon et al., 2004, 2009). MEM plants did not exhibit differences in starch accumulation with respect to the wild type in SD at moderate PFDs but contained very low levels of malate and fumarate. This SD metabolic phenotype is accentuated at low PFD where the levels of malate and fumarate were extremely low throughout the day and starch accumulated to higher levels in all MEM lines

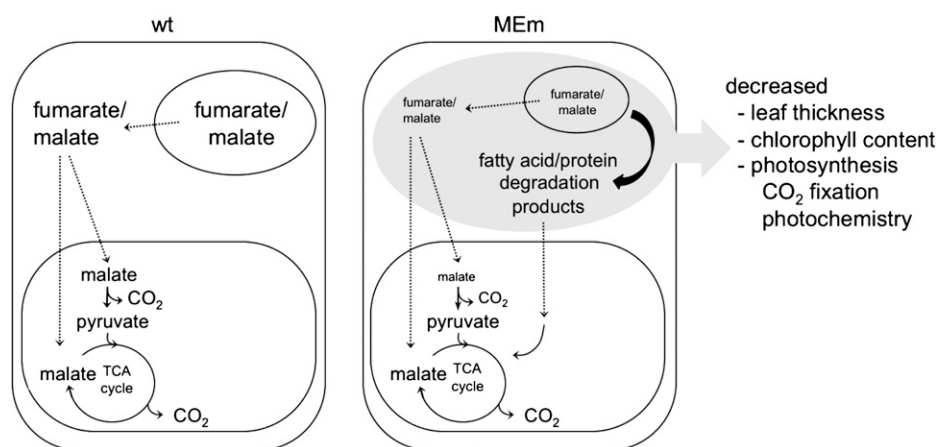


**Figure 6.** Model illustrating the changes observed in MEM plants growing in SD. At the end of a long night, the wild type (wt) uses organic acids to support respiration along with starch. The extremely low levels of malate and fumarate found in MEM plants may provide an initial signal (represented by the black file) generated after carbohydrate starvation at the end of the long night that induces the switch to use fatty acids and/or proteins for respiration. This carbon starvation (represented in gray) may trigger a cascade of events that result in morphological, biochemical, and physiological changes observed in the MEM plants growing in SD. Dashed files indicate transport processes.

compared to wild type (Fig. 3B). These results suggest that in MEM plants grown in low light a metabolic signal is sensed that triggers a higher rate of starch synthesis probably to counterbalance the limiting carbon supplies in the form of malate and/or fumarate, through a still unknown mechanism.

The analysis of the nature of the substrate supporting respiration indicated that LD wild-type and MEM plants use primarily carbohydrates as respiratory substrates at the end of the day and the night. The observed RQs in SD plants are also consistent with carbohydrates being the principal substrate supporting respiration by the end of the day in both wild-type and MEM plants. However, at the end of the night the wild type shift from carbohydrates to organic acids to support respiration, while MEM plants use fatty acids and/or proteins. These results clearly indicate that at the end of a long night the wild type uses organic acids due to a limitation of the carbon supply from the carbohydrate reserves. It was previously shown that *Arabidopsis* wild-type plants grown in progressively shortened photoperiods synthesize proportionally more starch in the light, degrade it more slowly during the night, and present progressively decreased levels of malate and fumarate at the end of the night (Gibon et al., 2004, 2009). Taken all together we propose that even though starch may not be completely consumed at the end of a long night, the organic acids, malate and fumarate, act as an alternative source of energy, which buffers the use of starch.

In MEM plants the superimposed shortage of carbon due to extremely low levels of malate and/or fumarate, especially at the end of a long night, exerts a limitation on metabolism, resulting in the catabolism of substrates from lipid and/or protein degradation. We postulate that in SD after using the permissible carbohydrate reserves, the MEM suffer from an acute carbon starvation (Fig. 6). This change occurring at the end of a long night would trigger the development of the pale-green phenotype reflected in decreased biomass and lowered photosynthetic capacity under this condition of growth (Fig. 1A).

## CONCLUSION

Our data demonstrate that although MEM plants grown under SD and LD regimes have some common differences in metabolite levels compared to wild type (see Fahnenstich et al., 2007 for data on LD), they only showed phenotypical differences when grown in SD. The fact that at the end of a long night the wild type use organic acids and the MEM plants use fatty acids and/or proteins as primary respiratory substrates, leads to the conclusion that the SD phenotype of MEM plants is a consequence of a long dark period with extremely low levels of malate and/or fumarate that are not sufficient to buffer the use of the carbohydrate reserves and thus cannot support normal metabolism after sugar depletion (Fig. 6). This clear

carbon-starvation phenotype of the SD transformants strengthens the proposed physiological roles of malate and fumarate as essential transient storage carbon molecules in a C<sub>3</sub>-plant-like *Arabidopsis*. Moreover, a superimposed reduced carbon gain during the day may also contribute to the pale-green thin leaves phenotype of the SD MEM plants. We propose that low levels of the organic acids may be the initial signal generated after carbohydrate starvation in the dark phase that triggers a cascade of events that alters use of reserves for respiration and chloroplast metabolism in the MEM plants (Fig. 6).

## MATERIALS AND METHODS

### Plant Material and Growth Conditions

After a cold treatment of 48 h at 4°C in the dark, *Arabidopsis* (*Arabidopsis thaliana*) ecotype Columbia-0 (wild type) and the transgenic lines (MEM2, -4, and -5; Fahnenstich et al., 2007) were grown in pots containing three parts soil (Gebr. Patzer KG) and one part vermiculite (Basalt Feuerfest) under LD conditions (16/8-h photoperiod) at a PFD of 75 or 150  $\mu\text{mol m}^{-2} \text{s}^{-1}$  or under SD conditions (8/16-h photoperiod) at a PFD of 30, 75, or 150  $\mu\text{mol quanta m}^{-2} \text{s}^{-1}$ . During the day the temperature was 22°C and during the night was 18°C.

### Measurement of Nucleotide Levels

Nucleotide levels were measured using total rosette harvested at the end of dark and light periods. The extraction and the contents of NADP, NADPH, NAD, and NADH were conducted as described in Matsumura and Miyachi (1980) and using the enzymatic cycling method of Lowry et al. (1961). To establish the efficiency of the extraction procedure, the recovery of nucleotides was determined by the addition of standard nucleotides (3-fold excess of the determined tissue concentration in the wild type) to the tissue sample at the start of the extraction procedure. Estimates of the recovery were 95% to 97% for all the nucleotides assayed.

### Determination of Metabolite Levels

Analysis of metabolites by GC-MS was performed by extraction and derivatization of 100 mg of whole rosettes from plants grown in SD as described previously (Fahnenstich et al., 2007). Substances were identified by comparison with standards and the recovery of small representative amounts of each metabolite through the procedure has been determined as described for the nucleotide measurements. Estimates of recovery were between 70% (for succinate) and 120% (for fumarate). Data sets presented are normalized to the wild-type control of each measured batch as a reference.

### Carbohydrates, Organic Acid, and Chlorophyll Quantification

The contents of starch, Glc, Fru, and Suc were determined enzymatically according to Stitt et al. (1989). Malate content was quantified photometrically using the combined assay as in Hurth et al. (2005). Chlorophyll quantification was carried out according to Arnon (1949).

### Light Microscopy

Samples for light microscopy were fixed overnight at 4°C in 2% formaldehyde (v/v), 1% glutaraldehyde, 50 mM NaPi, pH 7.2, and dehydrated with a graded ethanol series. For the determination of leaf thickness, the samples were embedded in Leica Histowax (Leica Microsystems) resin. The material was cut into 12- $\mu\text{m}$  sections. Leaf thickness was determined between the central and both outer lateral veins using the program Diskus (Hilgers). At least 80 sections, belonging to leaves of six different plants were used. Results were documented using a microscope Nikon eclipse E800 equipped with a digital camera (ky-F1030, JVC).

For leaf anatomy and starch staining leaf samples were fixed at 4°C in 2% (v/v) paraformaldehyde and 1.25% (v/v) glutaraldehyde in 0.05 M PIPES buffer, pH 7.2. The samples were dehydrated with a graded ethanol series and embedded in London Resin White (Electron Microscopy Sciences) acrylic resin. The periodic acid-Schiff's procedure was used for staining starch in sectioned materials. Cross sections (0.8–1 µm thick) were dried from a drop of water onto gelatin-coated slides, incubated in periodic acid (1% w/v) for 30 min, washed, and then incubated with Schiff's reagent (Sigma Aldrich) for 1 h. Controls lacking the periodic acid treatment showed little or no background staining (data not shown).

### Transmission Electron Microscopy

For chloroplast ultrastructure analysis leaves of 5-week-old plants growing in SD were used. Seedlings were fixed with 3% glutaraldehyde (v/v), 100 mM NaPi, pH 7.2 for 5 h, and washed three times with 100 mM NaPi. The samples were post fixed in 2% (w/v) osmium tetroxide for 4 h and washed three times with water. Samples were incubated in 25% (v/v) acetone for 20 min and subsequently in 50% acetone, 1% uranyl acetate for 2 h, followed by a sequential dehydration with 70%, 96%, and 100% acetone and embedded in Spurr's epoxy resin. Ultrathin sections were stained for transmission electron microscopy with 2% (w/v) uranyl acetate followed by 2% (w/v) lead citrate.

### Carbon Dioxide Assimilation and Chlorophyll Fluorescence Measurements

Measurements of CO<sub>2</sub> assimilation with varying C<sub>i</sub> were carried out using the LI-6400 system (LI-COR) and parameters were calculated with the software supplied by the manufacturer. Conditions were: PFD of 100, 150, or 200 µmol m<sup>-2</sup> s<sup>-1</sup>, chamber temperature of 24°C, flow rate of 100 µmol s<sup>-1</sup>, and a relative humidity of 60% to 70%.

Measurements of chlorophyll fluorescence of the upper leaf surface were performed with a PAM-2000 pulse amplitude modulation chlorophyll fluorometer (Walz GmbH; Schreiber et al., 1986). Basal fluorescence ( $F_0$ ) was measured with modulated weak red light using leaves, which were dark adapted for at least 10 min before giving a saturation pulse of light to obtain  $F_m$ . To calculate the  $F_v/F_m$  ratio, leaves were dark adapted for 10 min. The variable fluorescence ( $F_v$ ) was determined by subtracting  $F_0$  from  $F_m$ . Maximal fluorescence in the dark-adapted state ( $F_m$ ) and during illumination ( $F_m'$ ) was induced with a saturating white light pulse (5,000 µmol m<sup>-2</sup> s<sup>-1</sup>; duration 0.8 s). According to Genty et al. (1989) the effective quantum yield of PSII ( $\Phi_{PSII}$ ) was calculated as  $\Phi_{PSII} = (F_m' - F_s)/F_m'$  ( $F_s$  = steady-state fluorescence).

### RQ

The RQ (CO<sub>2</sub> eliminated/O<sub>2</sub> consumed) was determined by Warburg manometry (Braun-GmbH). Leaf discs were prepared 30 min before the end of the day and night from plants growing in SD and LD and the respiratory activity was measured for the next 75 min.

### Frequency Resolved Fluorescence Microscopy

The PSI to PSII ratio was determined by confocal stage scanning microscopy combined with frequency resolved fluorescence spectroscopy using leaves of 3-week-old plants grown either in SD and LD. Fluorescence was recorded from at least three different plants per condition. The measurements were performed with a custom-built confocal sample scanning microscope (based on a Zeiss Axiovert 135 TV, immersion oil objective: Zeiss Plan Neofluar 100/1.30 oil; Blum et al., 2001; Schleifenbaum et al., 2008) equipped with a 632.8 nm HeNe laser as source for excitation light (Polytec 610, Polytec GmVH). Fluorescence intensity images were obtained by raster scanning the sample and detecting emission intensity for every spot on the sampled area. At least 40 spots from regions exhibiting high and low overall fluorescence were addressed to record the corresponding fluorescence spectra. Acquisition time was 1 s per spectrum. Processing of fluorescence intensity images was accomplished with the WSxM software package (Nanotec Electronica; Horcas et al., 2007). PSI to PSII ratios were calculated from the corresponding spectra by dividing the fluorescence intensity maximum of PSI ( $I_{emPSI} = 740$  nm) by the fluorescence intensity maximum of PSII ( $I_{emPSII} = 680$  nm).

### Statistical Analysis

Significance was determined according to the Student's *t* test using Excel software (Microsoft Corporation) and the term significant is used only in the case that the change observed has a  $P < 0.05$ .

Sequence data from this article can be found in the GenBank/EMBL data libraries under accession number J05130.

### Supplemental Data

The following materials are available in the online version of this article.

**Supplemental Figure S1.** Specific leaf area of rosettes of 6-week-old wild-type (wt) and MEm plants grown in SD under different light regimes and 4-week-old plants in LD.

**Supplemental Figure S2.** Efficiency of PSII photochemistry: the effective quantum yield ( $\Phi_{PSII}$ ) as a function of the PFD (a) and time course of PSII inactivation ( $F_v/F_m$ ) during the course of high-light treatment (b).

**Supplemental Table S1.** Fresh weight (FW), dry weight (DW), and fresh weight/dry weight ratio (FW/DW) of rosettes of 6-week-old wild-type (wt) and MEm plants in SD and 4-week-old plants in LD following growth in different light regimes and light intensity conditions.

**Supplemental Table S2.** Total chlorophyll and chlorophyll *a* and *b* contents and chlorophyll *a/b* ratio of rosettes of 6-week-old wild-type and MEm plants grown in SD and 4-week-old plants grown in LD.

**Supplemental Table S3.** Relative distribution of thylakoids per granum (%) in chloroplasts of wild-type and MEm5 plants grown in LD and SD at moderate PFD.

**Supplemental Table S4.** Complete data set of metabolites measured by GC-MS over a day-night period from whole rosettes of plants grown in SD at a PFD of 150 µmol m<sup>-2</sup> s<sup>-1</sup>.

**Supplemental Table S5.** Complete data set of metabolites measured by GC-MS over a day-night period from whole rosettes of plants grown in SD at a PFD of 30 µmol m<sup>-2</sup> s<sup>-1</sup>.

### ACKNOWLEDGMENTS

We thank Alfred J. Meixner for the use of the fluorescence microscopy facility at IPTC (Tuebingen) and Kirstin Elgass, York-Dieter Stierhof, and Dagmar Ripper for excellent assistance.

Received December 1, 2009; accepted January 23, 2010; published January 27, 2010.

### LITERATURE CITED

- Arnon DI (1949) Copper enzymes in isolated chloroplasts: polyphenol oxidase in *Beta vulgaris*. *Plant Physiol* **24**: 1–15
- Becker B, Holtgreve S, Jung S, Wunrau C, Kandlbinder A, Baier M, Dietz KJ, Backhausen JE, Scheibe R (2006) Influence of the photoperiod on redox regulation and stress responses in *A. thaliana* L. (Heynh.) plants under long- and short-day conditions. *Planta* **224**: 380–393
- Blum C, Starcke F, Becker S, Mülle K, Meixner AJ (2001) Discrimination and interpretation of spectral phenomena by room-temperature single-molecule spectroscopy. *J Phys Chem* **105**: 6983–6990
- Chia DW, Tennessee JY, Retier WD, Gibson S (2000) Fumaric acid: and overlooked form of fixed carbon in *A. thaliana* and other plant species. *Planta* **211**: 743–751
- Drincovich ME, Lara M, Maurino VG, Andreo CS (2010) C<sub>4</sub> decarboxylases: different solutions for the same biochemical problem, the provision of CO<sub>2</sub> in the bundle sheath cells. In A Raghavendra, RF Sage, eds, C<sub>4</sub> Photosynthesis and Related CO<sub>2</sub> Concentrating Mechanisms. Advances in Photosynthesis and Respiration (AIPH) Series. Springer, Berlin (in press)
- Fahnstich H, Saigo M, Niessen M, Zanon MI, Andreo CS, Femie AR, Drincovich ME, Flügge UI, Maurino VG (2007) Alteration of organic

- acid metabolism in *A. thaliana* overexpressing the maize C<sub>4</sub>-NADP-malic enzyme causes accelerated senescence during extended darkness. *Plant Physiol* **145**: 640–652
- Fernie AR, Martinoia E** (2009) Malate: jack of all trades or master of a few? *Phytochemistry* **70**: 828–832
- Geiger DR, Servaites JC** (1994) Diurnal regulation of photosynthetic carbon metabolism in C3 plants. *Annu Rev Plant Biol* **45**: 235–256
- Genty B, Briantais JM, Baker NR** (1989) The relationship between the quantum yield of photosynthetic electron transport and the quenching of chlorophyll fluorescence. *Biochim Biophys Acta* **990**: 87–92
- Gibon Y, Bläsing O, Palacios N, Pankovic D, Hendriks JHM, Fisahn J, Höhne M, Günter M, Stitt M** (2004) Adjustment of diurnal starch turnover to short days: a transient depletion of sugar towards the end of the night triggers a temporary inhibition of carbohydrate utilization, leading to accumulation of sugars and post-translational activation of ADP glucose pyrophosphorylase in the following light period. *Plant J* **39**: 847–862
- Gibon Y, Pyl ET, Sulpice R, Lunn JE, Höhne M, Günter M, Stitt M** (2009) Adjustment of growth, starch turnover, protein content and central metabolism to a decrease of the carbon supply when *Arabidopsis* is grown in very short photoperiods. *Plant Cell Environ* **32**: 859–874
- Gout E, Bligny R, Pascal N, Douce R** (1993) <sup>13</sup>C Nuclear magnetic resonance studies of malate and citrate synthesis and compartmentation in higher plant cells. *J Biol Chem* **268**: 3986–3992
- Horcas I, Fernandez R, Gomez-Rodriguez JM, Colchero J, Gomez-Herrero J, Baro AM** (2007) WSXM: a software for scanning probe microscopy and a tool for nanotechnology. *Rev Sci Instrum* **78**: 013705
- Hugly S, Kunst L, Browse J, Somerville C** (1989) Enhance thermal tolerance of photosynthesis and altered chloroplast ultrastructure in a mutant of *A. thaliana* deficient in lipid desaturation. *Plant Physiol* **90**: 1134–1142
- Hurth MA, Suh SJ, Kretschmar T, Geis T, Bregante M, Gambale F, Martinoia E, Neuhaus HE** (2005) Impaired pH homeostasis in *A. thaliana* lacking the vacuolar dicarboxylate transporter and analysis of carboxylic acid transport across the tonoplast. *Plant Physiol* **137**: 901–910
- Koornneef A, Alonso-Blanco C, Peeters AJM, Soppe W** (1998) Genetic control of flowering time in *A. thaliana*. *Annu Rev Plant Physiol Plant Mol Biol* **49**: 345–370
- Lowry OH, Passonneau JV, Schulz DW, Rock MK** (1961) The measurement of pyridine nucleotides by enzymatic cycling. *J Biol Chem* **236**: 2746–2752
- Martinoia E, Rentsch D** (1994) Malate compartmentation-responses to a complex metabolism. *Annu Rev Plant Physiol Plant Mol Biol* **45**: 447–467
- Matsumura H, Miyachi S** (1980) Cycling assay for nicotinamide adenine dinucleotides. *Methods Enzymol* **69**: 465–470
- Maurino VG, Drincovich ME, Andreo CS** (1996) NADP-malic enzyme isoforms in maize leaves. *Biochem Mol Biol Int* **38**: 239–250
- Noctor G, Queval G, Gakière B** (2006) NAD(P) synthesis and pyridine nucleotide cycling in plants and their potential importance in stress conditions. *J Exp Bot* **57**: 1603–1620
- Oliver SN, Lunn JE, Urbanczyk-Wochniak E, Lytovchenko A, van Dongen JT, Faix B, Schmälzlin E, Fernie AR, Geigenberger P** (2008) Decreased expression of cytosolic pyruvate kinase in potato tubers leads to a decline in pyruvate resulting in an in vivo repression of the alternative oxidase. *Plant Physiol* **148**: 1640–1654
- Reiser J, Linka N, Lemke L, Jeblick W, Neuhaus HE** (2004) Molecular physiological analysis of the two plastidic ATP/ADP transporters from *A. thaliana*. *Plant Physiol* **136**: 3524–3536
- Schleifenbaum F, Blum C, Elgass K, Suramaniam V, Meixner AJ** (2008) New insights into the photophysics of DsRed by multiparameter spectroscopy on single proteins. *J Phys Chem* **112**: 7669–7674
- Schreiber U, Schliwa U, Bilger W** (1986) Continuous recording of photochemical and non-photochemical chlorophyll fluorescence quenching with a new type of modulation fluorometer. *Photosynth Res* **10**: 51–62
- Stitt M, Bulpin PV, ap Rees T** (1978) Pathway of starch breakdown in photosynthetic tissue of *Pisum sativum*. *Biochim Biophys Acta* **544**: 200–214
- Stitt M, Lilley RMC, Gerhardt R, Heldt HW** (1989) Determination of metabolite levels in specific cells and subcellular compartments of plant leaves. *Methods Enzymol* **174**: 518–522
- Stumpf DK, Burris RH** (1981) Organic acid contents of soybeans: age and source of nitrogen. *Plant Physiol* **68**: 989–991
- Sun J, Okita TW, Edwards GE** (1999) Modification of carbon partitioning, photosynthetic capacity, and O<sub>2</sub> sensitivity in *A. thaliana* plants with low ADP-glucose pyrophosphorylase activity. *Plant Physiol* **119**: 267–276
- Takeuchi Y, Akagi H, Kamasawa N, Osumi M, Honda H** (2000) Aberrant chloroplasts in transgenic rice plants expressing a high level of maize NADP-dependent malic enzyme. *Planta* **211**: 265–274
- Tronconi MA, Fahnenstich H, Gerrard Wheeler M, Andreo CS, Flügge UI, Drincovich ME, Maurino VG** (2008) *Arabidopsis thaliana* NAD-malic enzyme functions as homodimer and heterodimer and has a major impact on nocturnal metabolism. *Plant Physiol* **146**: 1540–1552
- Vanlerberghe GC, Yip JYH, Parsons HL** (1999) In organelle and in vivo evidence of the importance of the regulatory sulfhydryl/disulfide system and pyruvate for alternative oxidase activity in tobacco. *Plant Physiol* **121**: 793–803
- Zabalza A, van Dongen JT, Froehlich A, Oliver SN, Faix B, Gupta KJ, Schmälzlin E, Igal M, Orcaray L, Royuela M, et al** (2009) Regulation of respiration and fermentation to control the plant internal oxygen concentration. *Plant Physiol* **149**: 1087–1098
- Zeeman SC, ap Rees T** (1999) Changes in carbohydrate metabolism and assimilate export in starch-excess mutants of *A. thaliana*. *Plant Cell Environ* **22**: 1445–1453
- Zeeman SC, Smith SM, Smith AM** (2007) The diurnal metabolism of leaf starch. *Biochem J* **401**: 13–28